An Accurate Technique for Array Design and Characterization in MIMO Channel

Celal Alp Tunc, Vakur B. Ertürk, Defne Aktas, and Ayhan Altintas

Department of Electrical and Electronics Engineering, Bilkent University,
Bilkent, Ankara, 06800, Turkey (e-mail: celal@ee.bilkent.edu.tr).

Abstract

A full-wave analysis technique based on the method of moments solution of the electric field integral equation is presented to evaluate the MIMO channel matrix accurately by including majority of electromagnetic effects. Effects of mutual interactions among the array elements through space and surface waves (in the case of printed arrays) are included in the channel matrix. Besides achieving the accuracy, various comparisons can be made among arrays of linear wire, printed dipole and rectangular patch antennas. Effects of array characterization on the communication system performance are analyzed, in terms of electrical and geometrical properties such as dielectric thickness, permittivity and termination impedances. The computational efficiency of the technique allows us to analyze MIMO performance of arrays with large number of antennas and high performance array design in conjunction with well-known optimization tools. Moreover, considering many parasitic array elements as near field scatterers, the MIMO capacity boost in poor multipath environments or even under line-of-sight (LOS) conditions is investigated with the help of the technique.

1. Introduction

Multiple Input Multiple Output (MIMO) wireless communication systems have been a focus of interest, due to their ability to increase the capacity in rich scattering environments by using multi-element antenna (MEA) arrays both at the transmitter and the receiver sides [1, 2]. The choice of MEA array type and configuration may affect the wireless channel behavior significantly. Therefore, transmitter and receiver antennas must be incorporated into the wireless channel model by including as many electromagnetic effects as possible to have a better system design. In this paper we present a full-wave electromagnetic model with electric fields (MEF), to evaluate the MIMO channel matrix accurately by including majority of the electromagnetic effects when desired. The presented technique includes the effects of mutual interactions among the array elements through space and surface waves (when printed arrays are considered) using a full-wave method of moments (MoM)/Green's function method. The stochastic nature of the approach is due to a local cluster of scatterers. Consequently, the presented method is deterministic and exact except the scatterer scenario. Thus, besides achieving the accuracy, various comparisons can be made among arrays of linear wire, printed dipole and rectangular patch antennas. Furthermore, the presented MEF is computationally efficient yielding accurate results.

In this paper, the formulation of the technique and sample numerical results on a MIMO performance comparison of a freestanding linear dipole array with a printed one are given, in terms of channel capacity, correlations and received signal to noise ratio. Investigations with the aid of the technique on the following are being performed and the results will be presented in the conference session: (*i*) array characterization effects on the communication system performance, regarding electrical and geometrical properties such as dielectric thickness and permittivity, (*ii*) high performance array design in conjunction with well-known particle swarm optimization tool, (*iii*) the MIMO capacity boost in poor multipath environments or even under LOS conditions, considering many parasitic array elements as near field scatterers. An $e^{j\omega t}$ time convention is used and suppressed from the expressions, where ω is the angular frequency.

2. MIMO Channel Model with Electric Fields

The scattering environment is a two dimensional (2D), single-bounce geometric model. It assumes a transmitter (TX) and a receiver (RX) array, and a local cluster of scatterers around TX. The local cluster is a disk of radius R_D including S uniformly distributed scatterers. Note that, the use of any other geometrical scatterer scenario is possible in conjunction with MEF, as well. Assuming flat fading, the received signal vector, $\bar{V}^{rx}$, can be written in terms of the transmitted one, $\bar{V}^{tx}$, and the additive white Gaussian noise vector, $\bar{n}$, with zero mean independent identically distributed (i.i.d.) elements with unit variance as in (1). In (1), $\mathbf{H}$ denotes the $R \times T$ channel matrix, where R and T are the number of antenna elements in receiver and transmitter arrays, respectively. Assuming channel knowledge only

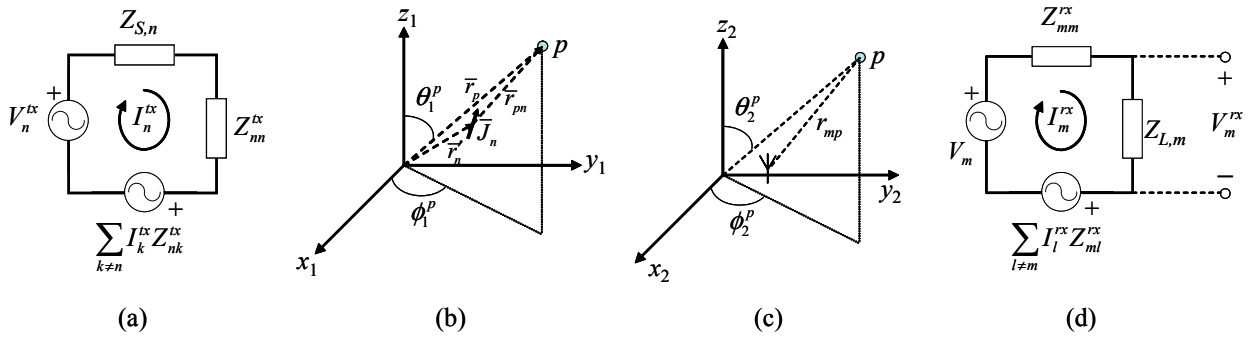

Figure 1: (a) Circuit model of the nth transmit element. (b) Geometry of the nth transmit element and pth scatterer. (c) Geometry of the mth receive element and pth scatterer. (d) Circuit model of the mth receive element.

at the receiver side, the maximum amount of data transmitted reliably (i.e., the Shannon capacity) can be evaluated as in (2), where $\mathbf{I}$ is the $R \times R$ identity matrix, $|.|$ is the matrix determinant, $P_T = E[\bar{V}^{tx*}\bar{V}^{tx}]$ is the total transmitted power with $(.)^*$ and $E[.]$ denoting the conjugate transpose and expectation operations, respectively.

$$\bar{V}^{rx} = \mathbf{H}\,\bar{V}^{tx} + \bar{n}. \tag{1}$$

$$\mathcal{C} = \log_2\left(\left|\mathbf{I} + \frac{P_T}{T}\mathbf{H}\mathbf{H}^*\right|\right) \tag{2}$$

$$\bar{I}^{tx} = \left(\mathbf{Z}^{tx} + \mathbf{Z}_S\right)^{-1}\bar{V}^{tx} \tag{3}$$

$$\bar{E}_{np} = \frac{-j\omega\mu_0}{4\pi}\int_{S_n} \bar{J}_n(\bar{r}_n')\,G(\bar{r}_p,\bar{r}_n')\,dr_n'. \tag{4}$$

$$\bar{E}_p = \sum_{n=1}^{T}\bar{E}_{np} = \hat{\theta}_1^p\,E_{p,\theta} + \hat{\phi}_1^p\,E_{p,\phi} \tag{5}$$

$$V_{p,\theta}^{0} = \alpha_p^{\theta\theta}E_{p,\theta} + \alpha_p^{\theta\phi}E_{p,\phi} \tag{6}$$

$$V_{p,\phi}^{0} = \alpha_p^{\phi\theta}E_{p,\theta} + \alpha_p^{\phi\phi}E_{p,\phi} \tag{7}$$

$$\bar{E}_{pm} = \left(\hat{\theta}_2^p\,V_{p,\theta}^{0} + \hat{\phi}_2^p\,V_{p,\phi}^{0}\right)\frac{e^{-jkr_{mp}}}{r_{mp}} \tag{8}$$

$$E_m = \sum_{p=1}^{S}\hat{u}_m\cdot\bar{E}_{pm} \tag{9}$$

$$\bar{V}^{rx} = \mathbf{Z}_L\left(\mathbf{Z}^{rx} + \mathbf{Z}_L\right)^{-1}\bar{V} \tag{10}$$

$$V_m = \int_{S_m} E_m(r_m')\,w_m(r_m')\,dr_m' \tag{11}$$

Fig. 1 (a) shows the circuit model for the nth antenna element of the transmit array [3]. The MoM interactions matrix of the TX array, $\mathbf{Z}^{tx}$, relates the currents on the array elements, $\bar{I}^{tx}$, with the source voltages, $\bar{V}^{tx}$, via (3), where $\mathbf{Z}_S$ is a diagonal matrix, non-zero entries of which are the source impedances of each transmit element. The incident electric field on the pth scatterer in the far zone of the TX array due to the nth transmitter antenna is given by (4). In (4), μ_0 denotes the magnetic permeability of free space, $\bar{J}_n$ is the current density on the nth TX element due to I_n^{tx}, and $\int_{S_n} dr_n'(\cdot)$ is the surface integration over the element. In addition, $G(\bar{r}_p,\bar{r}_n')$ represents the Green's function of the environment, where $\bar{r}_p$ and $\bar{r}_n'$ are the position vectors pointing the pth scatterer and nth TX antenna, respectively.

The total incident field on the pth scatterer from TX array is obtained as in (5), where $\hat{\theta}_1^p$ and $\hat{\phi}_1^p$ are the unit normal vectors due to elevation and azimuth angles of the pth scatterer in the spherical coordinate system, whose origin coincides with the center of the TX array, as illustrated in Fig. 1 (b). Each scatterer is assumed to have a 2×2 scattering coefficient matrix, $\mathbf{A}_p$, whose entries ($\alpha_p^{\theta\theta}$, $\alpha_p^{\theta\phi}$, $\alpha_p^{\phi\theta}$, $\alpha_p^{\phi\phi}$) are i.i.d. Gaussian random variables with zero mean and unit variance. Assuming each scatterer as an isotropic radiator, the cross-polarized field scattered from the pth scatterer impinging on the mth receiver antenna, $\bar{E}_{pm}$, can be expressed as in (6)-(8); where k denotes the free space propagation constant and r_{mp} is the distance between the mth RX element and pth scatterer.

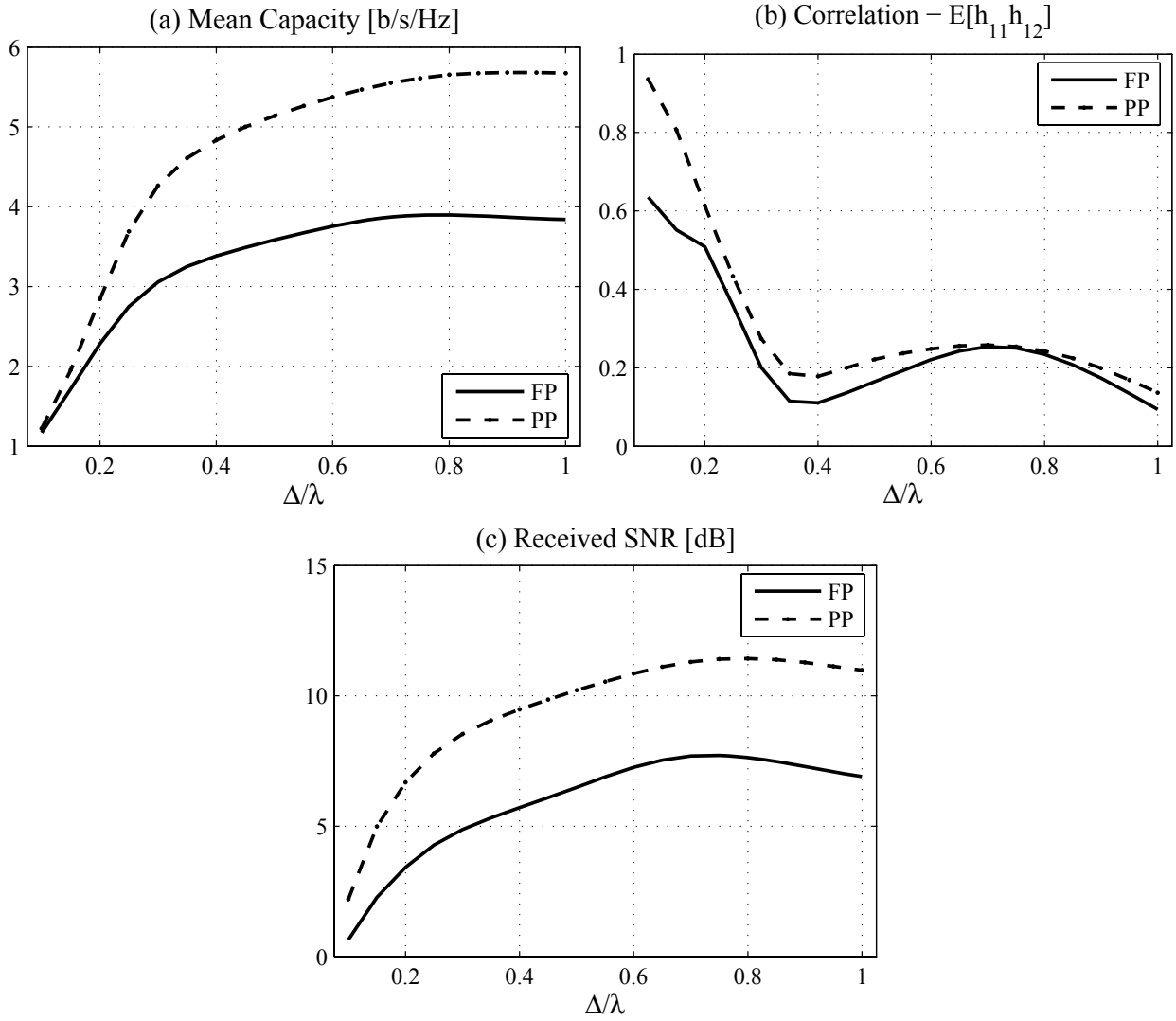

Figure 2: MIMO performance comparison of PLDA with FLDA versus interelement spacing. PP: Identical PLDA located both at TX and RX. FP: FLDA at TX and PLDA at RX (a) Mean capacity. (b) Correlation. (c) Received SNR.

Note that, in (8), the unit normal vectors $(\hat{\theta}_2^p,\ \hat{\phi}_2^p)$ are chosen for a different spherical coordinate system, whose origin coincides with the center of the RX array, as shown in Fig. 1 (c). Total field received by the mth receiver element is given by (9), where $\hat{u}_m$ is the unit normal vector denoting the polarization direction of the element. Making use of the circuit model [3] of the mth receiver element depicted in Fig. 1 (d), the received signal vector, $\bar{V}^{rx}$, is obtained from the system of linear equations given by (10), where $\mathbf{Z}^{rx}$ is the mutual interactions matrix of the RX array obtained via MoM, $\mathbf{Z}_L$ is the load impedances matrix (which is diagonal), and $\bar{V}$ is the excitation vector of the MoM matrix equation obtained from the total received fields on RX elements. The entries of $\bar{V}$ are evaluated by (11), where w_m is the weighting function over the mth receiver element and taken as the current distribution on the element (i.e., mth testing function) to employ a Galerkin's MoM solution.

In order to find the entries of mutual coupling included $\mathbf{H}$, the following procedure of MEF is presented: (*i*) Evaluate $\mathbf{Z}^{tx}$ and $\mathbf{Z}^{rx}$. (*ii*) Start with $n = 1$. (*iii*) Activate nth TX element ($V_n^{tx} = 1\text{V},\ V_{k\neq n}^{tx} = 0$). (*iv*) Calculate the current vector utilizing (3). (*v*) Evaluate (4)-(11); then, the entries of the MIMO channel matrix can be simply evaluated as $h_{mn} = V_m^{rx}$. (*vi*) Increase n, and go to (*iii*).

3. Numerical Results

Using the presented MEF approach, performances of linear arrays of freestanding and printed dipole elements are investigated in terms of mean channel capacity, received signal to noise ratio (SNR) and channel correlation. The scenario is formed by locating $S = 100$ uniformly distributed scatterers around the transmitter within a disk of radius of $R_D = 200\lambda$, on the plane perpendicular to the direction of the current on antenna elements. Transmit and receive arrays are assumed to be located 300λ away from each other in a broadside manner, formed by $R = T = 2$ uniform dipoles, where the interelement spacing for both arrays is Δ. Results are generated for different Δ values between 0.1λ and λ. In the results, the transmit power (P_T) is fixed for all Δ values. Mean capacity results are obtained by averaging the MIMO channel capacity over $N_R = 1000$ channel realizations. PLDA analyzed here are formed by uniform dipoles of $\lambda/2$ height and $\lambda/100$ width, which are placed on top of a dielectric substrate with a dielectric constant of $\epsilon_r = 3.25$ and a thickness of $d = 0.06\lambda$ above a ground plane. Whereas, FLDA are considered to be composed of thin wire dipole elements of $\lambda/2$ height and $\lambda/200$ radius. Conjugate matching is applied at the terminals in all cases.

Fig. 2 compares the MIMO performance of PLDA with that of FLDA. First, identical PLDA with 2 side-by-side dipoles are located both at TX and RX. Then, a MIMO system with an FLDA at TX and a PLDA at RX is considered. MIMO performances are investigated in terms of the mean capacity (a), correlation (b) and received SNR per RX branch (c) versus interelement spacing (Δ). As expected, for small interelement spacings, the effect of mutual coupling reduces the capacity. The use of FLDA reduces the capacity due to decreased received SNR even though the correlation is lower. The reason behind this result is that, the radiation impedance (i.e., $\mathcal{R}e\{Z_{nn}\}$) of a printed dipole is less than that of a freestanding one, leading to more current on elements and more radiated power for fixed activation voltage under conjugate matching.

4. Conclusions

A model with electric fields based on MoM/Green's function technique is presented and used in order to accurately evaluate the MIMO channel matrix. The presented method is deterministic and exact except the scatterer scenario. Besides achieving accuracy, comparisons can be made among arrays of linear wire, printed dipole and rectangular patch antennas. Using the presented approach, performances of linear arrays of freestanding and printed dipole elements are compared. Our results on array characterization effects on the communication system performance, high performance array design in conjunction with particle swarm optimization, the MIMO capacity boost in poor multipath environments considering parasitic array elements as near field scatterers, will be presented in the conference session.

5. Acknowledgements

This work has been supported by the Turkish Scientific and Technical Research Agency (TÜBİTAK) under Grants EEEAG-106E081, EEEAG-104E044 and EEEAG-105E065; also in part by the European Union Network of Excellence (NoE) NewCom++, under the 7th Framework Programme.

6. References

1. I. E. Telatar, "Capacity of multi-antenna Gaussian channels," *Europ. Trans. Telecommun.*, vol. 10, pp. 585–595, Nov. 1999.

2. G. J. Foschini and M. J. Gans, "On limits of wireless communications in a fading environment when using multiple antennas," *Wireless Personal Commun.*, vol. 6, pp. 311–335, Mar. 1998.

3. J. Andersen and B. K. Lau, "On closely coupled dipoles in a random field," *IEEE Antennas Wireless Propagat. Lett.*, vol. 5, no. 1, pp. 73–75, 2006.